Tyrosine replacement in P-selectin glycoprotein ligand-1 affects distinct kinetic and mechanical properties of bonds with P- and L-selectin

Vishwanath Ramachandran*, Matthias U. Nollert†, Haiying Qiu‡, Wen-Jun Liu*, Richard D. Cummings‡, Cheng Zhu§, and Rodger P. McEver*‡¶‖

*W. K. Warren Medical Research Institute and Department of Medicine, ‡Department of Biochemistry and Molecular Biology, University of Oklahoma Health Sciences Center, and ¶Cardiovascular Biology Research Program, Oklahoma Medical Research Foundation, Oklahoma City, OK 73104; †School of Chemical Engineering and Materials Science, University of Oklahoma, Norman, OK 73019; and §George W. Woodruff School of Mechanical Engineering and Department of Biomedical Engineering, Georgia Institute of Technology, Atlanta, GA 30332

Edited by Stuart A. Kornfeld, Washington University School of Medicine, St. Louis, MO, and approved September 9, 1999 (received for review August 16, 1999)

Selectins are adhesion molecules that initiate tethering and rolling of leukocytes on the vessel wall. Rolling requires rapid formation and breakage of selectin–ligand bonds that must have mechanical strength to resist premature dissociation by the forces applied in shear flow. P- and L-selectin bind to the N-terminal region of P-selectin glycoprotein ligand-1 (PSGL-1), a mucin on leukocytes. To define determinants on PSGL-1 that contribute to the kinetic and mechanical properties of bonds with selectins, we compared rolling of transfected preB cells expressing P- or L-selectin on transfected cell monolayers expressing wild-type PSGL-1 or PSGL-1 constructs with substitutions in targeted N-terminal residues. Rolling through P- or L-selectin required a Thr or Ser at a specific position on PSGL-1, the attachment site for an essential O-glycan, but required only one of three nearby Tyr residues, which are sites for Tyr-SO_3 formation. The adhesive strengths and numbers of cells rolling through P- or L-selectin were similar on wild-type PSGL-1 and on each of the three PSGL-1 constructs containing only a single Tyr. However, the cells rolled more irregularly on the single-Tyr forms of PSGL-1. Analysis of the lifetimes of transient tethers on limiting densities of PSGL-1 revealed that L-selectin dissociated faster from single-Tyr than wild-type PSGL-1 at all shears examined. In sharp contrast, P-selectin dissociated faster from single-Tyr than wild-type PSGL-1 at higher shear but not at lower shear. Thus, tyrosine replacements in PSGL-1 affect distinct kinetic and mechanical properties of bonds with P- and L-selectin.

The initial step in leukocyte accumulation during inflammation is a rolling interaction on the blood vessel wall. This adhesive event is primarily mediated by binding of the selectins to cell-surface glycoconjugates that must be modified with sialic acid, fucose, and in some cases, sulfate (1, 2). L-selectin, expressed on most leukocytes, binds to ligands on endothelial cells and other leukocytes. P- and E-selectin, expressed on activated platelets and/or endothelial cells, bind to ligands on leukocytes and some endothelial cells.

Cell rolling is a dynamic process that requires the rapid formation and breakage of adhesive bonds that are subjected to hydrodynamic force in shear flow (3). Both the kinetic and mechanical properties of selectin–ligand interactions affect rolling adhesion (4). Biochemical and biophysical studies indicate that the dissociation rate, or k_{off}, for L-selectin–ligand bonds is 7- to 10-fold higher than for P-selectin or E-selectin bonds (5, 6). However, the mechanical strength of L-selectin bonds, i.e., their ability to resist accelerated dissociation by force, is greater than that of P- or E-selectin bonds. The structural features that dictate the kinetic and mechanical properties of selectin–ligand interactions are not understood. Mild periodate treatment cleaves the exocyclic C8 and C9 carbons from sialic acids on the mucin CD34 and markedly increases the mechanical strength of its interaction with L-selectin (7). However, it is not known whether periodate directly affects sialic acids in the binding site or indirectly affects the global flexibility of the mucin.

The best characterized selectin ligand is P-selectin glycoprotein ligand-1 (PSGL-1), a homodimeric mucin on leukocytes that binds to all three selectins (reviewed in ref. 8). mAbs that recognize N-terminal epitopes on PSGL-1 block rolling of leukocytes on P-selectin and significantly inhibit L-selectin-dependent rolling of leukocytes on other leukocytes (9, 10). The N terminus of mature human PSGL-1 begins at residue 42 as a result of cleavage of a signal peptide and propeptide during biosynthesis (11). Analysis of recombinant mutants of PSGL-1 suggests that P-selectin binds to a small N-terminal region of PSGL-1 that requires two distinct posttranslational modifications: sulfation of tyrosines clustered at residues 46, 48, and 51, and attachment of a core-2 O-glycan capped with sialyl Lewis x (sLe^x) (NeuAcα2,3Galβ1,4[Fucα1,3]GlcNAcβ1-R) at Thr-57 (12–16). These binding requirements have been unequivocally demonstrated by synthesis of a synthetic glycosulfopeptide containing residues 42–63 of PSGL-1 that is sulfated on all three tyrosines and has a short core-2 O-glycan capped with sLe^x at Thr-57 (17). This glycosulfopeptide binds to P-selectin with high affinity, but only if it has both the tyrosine sulfates and the core-2 O-glycan.

The number of tyrosine sulfates required for optimal binding of PSGL-1 to P-selectin has not been determined. Transfected preB cells expressing P-selectin roll on recombinant forms of PSGL-1 in which any two of the three tyrosines are substituted with phenylalanine (16). However, it was not determined whether specific parameters of P-selectin-dependent rolling on the single-Tyr PSGL-1 molecules were altered. Indirect evidence suggests that L-selectin also binds to an N-terminal region of PSGL-1 that requires tyrosine sulfation and specific O-glycosylation (10, 18). However, the number of tyrosines required for binding has not been determined, and the specific role of Thr-57, the putative site for attachment of a critical core-2 O-glycan, has not been addressed. It is particularly important to determine the structural features that contribute to binding of selectins to their ligands in shear flow in which the kinetic and mechanical properties of the bonds are essential to their functions.

This paper was submitted directly (Track II) to the PNAS office.

Abbreviations: C2GnT, core-2 β1,6-N-acetylglucosaminyltransferase; CHO, Chinese hamster ovary; Fuc-TVII, fucosyltransferase VII; PSGL-1, P-selectin glycoprotein ligand-1; sLe^x, sialyl Lewis x.

‖To whom reprint requests should be addressed at: W. K. Warren Medical Research Institute, University of Oklahoma Health Sciences Center, 825 N.E. 13th Street, Oklahoma City, OK 73104. E-mail: rodger-mcever@ouhsc.edu.

The publication costs of this article were defrayed in part by page charge payment. This article must therefore be hereby marked "*advertisement*" in accordance with 18 U.S.C. §1734 solely to indicate this fact.

In this paper, we directly compared the tethering and rolling of preB cells expressing P- or L-selectin on transfected cell monolayers expressing wild-type PSGL-1 or PSGL-1 constructs with substitutions in Thr-57 or in N-terminal tyrosine residues. PSGL-1 appears to require similar N-terminal posttranslational modifications to bind both selectins. However, limited tyrosine replacements in the binding domain of PSGL-1 reveal remarkable differences in the kinetic and mechanical properties of interactions with P- and L-selectin.

Materials and Methods

Cell Transfections. The cDNAs encoding wild-type human PSGL-1 and PSGL-1 constructs with amino acid substitutions in the N-terminal region were ligated into pZeoSV, which allows selection for cells resistant to Zeocin (Invitrogen) (16). The cDNA for α1,3-fucosyltransferase VII (Fuc-TVII) (19) was transferred from pCDM8 to pRc/RSV (Invitrogen), which allows selection for cells resistant to G418. The cDNA for core-2 β1,6 *N*-acetylglucosaminyltransferase (C2GnT) (15) was ligated into the *Kpn*I and *Xho*I site of pCEP4 (Invitrogen), which allows selection for cells resistant to hygromycin.

DHFR(−) Chinese hamster ovary (CHO) cells (American Type Culture Collection) were transfected with cDNAs for both Fuc-TVII and C2GnT using LipofectAMINE (Life Technologies, Gaithersburg, MD). Clones of transfected cells resistant to both G418 and hygromycin were selected for high activities of Fuc-TVII and C2GnT by flow cytometry. Fuc-TVII activity was measured by binding of the anti-sLe^x mAb CSLEX-1 (9). Expression of core-2 O-glycans was measured by binding of the anti-T antigen mAb, a gift from George F. Springer (Chicago Medical School, Chicago), to CHO cells previously desialylated by treatment with 5 milliunits of sialidase from *Arthrobacter ureafacians* (Boehringer Mannheim) for 30 min at 37°C. The anti-T mAb binds to desialylated core-1 O-glycans but not desialylated core-2 O-glycans. Therefore, much less anti-T mAb binds to CHO cells expressing high C2GnT activity. A clone of CHO cells expressing high levels of both sLe^x and core-2 O-glycans was transfected with cDNAs for wild-type PSGL-1 or mutant PSGL-1 constructs using electroporation. Transfected cells resistant to G418, hygromycin, and Zeocin were selected for matched, uniform expression levels of PSGL-1 by flow cytometry using anti-PSGL-1 mAbs PL1 and PL2 (9).

Transfected murine L1–2 preB cells expressing human P-selectin or L-selectin (20, 21) were a gift from Takashi Kei Kishimoto (Boehringer Ingelheim Pharmaceuticals).

Cell Accumulation, Shear Resistance, and Tethering in Shear Flow. L1–2 cells expressing P- or L-selectin (10^6/ml in Hanks' balanced salt solution plus 0.1% human serum albumin) were perfused over transfected CHO cell monolayers in 35-mm dishes mounted in a parallel-plate flow chamber at wall shear stresses ranging from 0.5 to 2 dyn/cm^2 (1 dyne = 10 μN) (16). The accumulated number of rolling cells was measured after 4 min of perfusion by using a videomicroscopy system coupled to a digital image analysis system (Inovision, Durham, NC) on a Silicon Graphics (Mountain View, CA) workstation. For each experiment, adherent cells in 10–12 fields were counted with a 20× objective. In some experiments, the L1–2 cells were preincubated with 20 μg/ml the anti-L-selectin mAb DREG-56 (22) or the anti-P-selectin mAb G1 (23), or the CHO cells were preincubated with 20 μg/ml the anti-PSGL-1 mAbs PL1 or PL2. The cells were perfused through the chamber in the continued presence of the antibody. To measure resistance to detachment under shear, P-selectin- or L-selectin L1–2 cells were allowed to accumulate at 0.5 or 1 dyn/cm^2, respectively, and cell-free buffer was then introduced. Wall shear stress was increased every 30 s, and the percentage of cells remaining adherent was determined. The rate at which free-flowing cells first tethered to the CHO cell monolayer was measured during the first 60 s of perfusion. The tethering rate at different wall shear stresses was normalized by dividing by the number of cells transported across the field of view in the focal plane of the monolayer.

Measurement of Velocities and Distances Traveled. Velocities of rolling cells were measured by tracking an individual cell frame-by-frame, or every 0.033 s, in the direction of flow (Nanotrack software; Inovision). For each selectin–PSGL-1 interaction, at least 20 L1–2 cells were tracked, each for up to 5 s, to yield a total observation time of ≥100 s. Rarely, cells attached irreversibly to the monolayer; these interactions were not selectin-dependent, because mAbs to P- or L-selectin or to PSGL-1 did not cause them to detach. At the wall shear stresses examined (0.5–2 dyn/cm^2), the velocities of these stationary cells measured over a 5-s interval were approximately normally distributed, with a nearly zero mean and an SD of ≈2 μm/s. Greater than 97% of the velocities measured at each video frame were <6 μm/s. This suggests that the overall measurement error for displacement of a cell between two successive frames is <0.2 μm. Therefore, 6 μm/s was used as an operational threshold to separate paused from rolling cells in each video frame. Each distance traveled by a rolling cell between two pauses was defined as the distance spanned during one continuous sequence of velocities greater than 6 μm/s. The distribution of distances traveled was plotted at each wall shear stress. The percentage of long distances traveled (>10 μm for P-selectin and >28 μm for L-selectin) was plotted for the interaction with wild-type or single-Tyr PSGL-1 as a function of wall shear stress. Assuming that errors for individual displacements are independent, the cumulative error was calculated as 0.2 μm times the square root of the number of frames for each distance traveled. Two additional histograms for distances traveled plus or minus cumulative errors were plotted. The difference between the two histograms and the previous one for each bin was taken as the error bar for that bin; the error bars were included in the final histogram.

Determination of Dissociation Rate Constants and Mechanical Strength of Selectin-PSGL-1 Bonds from Transient Tethering Events. Transient tether durations were determined by pretreating the CHO cell monolayers with a subsaturating (0.5 μg/ml) concentration of the blocking anti-PSGL-1 mAb PL1. Under these conditions, >98% of interactions of P- or L-selectin L1–2 cells with the monolayer were transient, i.e., the cells detached before they began to roll. The remaining cells rolled for ≤1 s before detaching. The duration of transient tethers was measured with an imaging system that has a time resolution of 0.033 s. Sufficient videotape to visualize 500-1000 tethering events was analyzed, and the natural log of the number of cells that remained bound as a function of time after initiation of tethering was plotted. For first-order dissociation kinetics, the resultant plot is a straight line, and the slope is $-k_{off}$. Five independent measurements of k_{off} were made for the interaction of P- or L-selectin L1–2 cells with each PSGL-1 construct at each wall shear stress examined. The dependence of k_{off} on applied force was assumed to follow the Bell equation (24): $k_{off} = k^0_{off} \exp(aF_b/kT)$, where k^0_{off} is the dissociation rate in the absence of applied force, a is the reactive compliance, F_b is the force on the bond, k is Boltzman's constant, and T is the absolute temperature. The force on the bond was calculated (25) using a diameter for L1–2 cells of 12 μm and assigning a bond angle of 50°. The Bell equation was fit to the k_{off} vs. F_b data using the exponential curve-fitting function in EXCEL (Microsoft), which returns the best-fit parameter values for k^0_{off} and a. The mean and SD from all five experiments was then calculated. Statistical significance was assessed by using Student's t test for unpaired analyses to compare the mean values of k^0_{off} and a for the interaction of wild-type and mutant forms of PSGL-1 with each selectin. The method of maximum likeli-

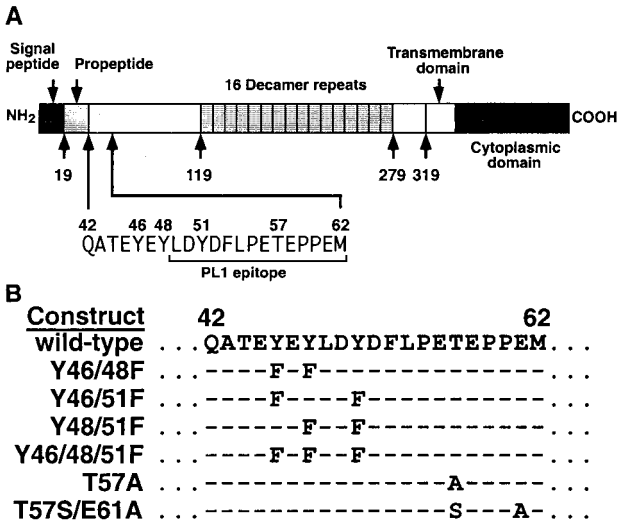

Fig. 1. Schematic diagram of human PSGL-1 constructs. (*A*) Diagram of the domains in wild-type PSGL-1, which self-associates to form homodimers in the membrane. The residue number that begins each region of the extracellular and transmembrane domains is indicated. The N terminus of mature PSGL-1 begins at residue 42, immediately after the propeptide. The sequence of the first 21 amino acids of mature PSGL-1 is listed. The epitope for the blocking anti-PSGL-1 mAb PL1 (30) is bracketed. Shown are the three consensus tyrosine sulfation sites at residues 46, 48, and 51, as well as Thr-57, a site for attachment for an O-glycan. (*B*) Sequences of the amino acid substitutions in the full-length PSGL-1 constructs.

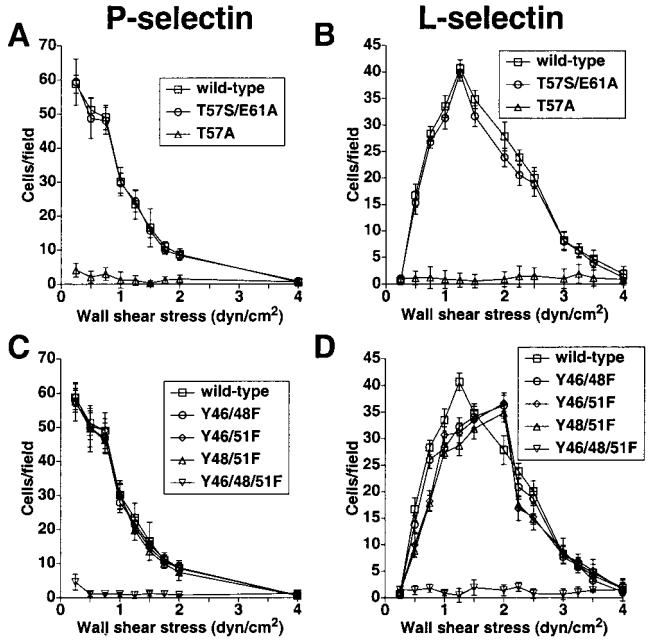

Fig. 2. Accumulation of rolling cells expressing P- or L-selectin on PSGL-1 constructs. L1–2 cells expressing human P-selectin (*A* and *C*) or L-selectin (*B* and *D*) were perfused at the indicated wall shear stress over CHO cell monolayers expressing Fuc-TVII, C2GnT, and the indicated PSGL-1 construct. After 4 min of perfusion, the number of L1–2 cells rolling on the monolayer was quantified. The data represent the mean ± SD of five experiments.

hood (26) was used as an independent procedure to determine k^0_{off} and a for the interaction of each selectin with each PSGL-1 construct and to determine the statistical significance of their differences. Data points with short tether durations are more heavily weighted after using the natural log to convert the exponentially distributed data to a linear plot. In contrast, the method of maximum likelihood weights all data points identically. Statistical significance with both methods was assumed for $P < 0.05$.

Results

Rolling of L1–2 Cells Expressing P- or L-Selectin on CHO Cells Expressing PSGL-1 Constructs. We previously prepared a series of cDNA constructs in which we altered selected amino acids in the N-terminal region of full-length human PSGL-1 (16) (Fig. 1). Each cDNA was transfected into CHO cells that had been stably transfected with cDNAs expressing C2GnT and Fuc-TVII. Cell sorting was used to obtain cells that expressed comparable levels of wild-type or mutant PSGL-1. Similar activities of C2GnT and Fuc-TVII in each clone were confirmed by flow cytometry with mAbs to the T antigen and the sLe^x determinant, respectively (data not shown).

We compared the rolling adhesion of transfected preB L1–2 cells expressing human P- or L-selectin on CHO cell monolayers expressing each of the PSGL-1 constructs at matched densities. Rolling required a specific interaction of the N-terminal region of PSGL-1 with P- or L-selectin, because it was blocked by a saturating concentration of mAb PL1 to PSGL-1 or by mAb G1 to P-selectin or mAb DREG-56 to L-selectin. Furthermore, little or no rolling was observed on parental CHO cells expressing C2GnT and Fuc-TVII without PSGL-1 (data not shown).

The accumulated number of P-selectin L1–2 cells rolling on wild-type PSGL-1 declined as wall shear stress was increased (Fig. 2*A*). Consistent with previous results (16), P-selectin L1–2 cells rolled on a PSGL-1 construct in which Thr-57 was replaced with Ser but not on a construct in which Thr-57 was replaced with Ala. L-selectin L1–2 cells required a minimum wall shear stress of ≈0.5 dyn/cm^2 to roll on wild-type PSGL-1 (Fig. 2*B*), confirming previous observations for L-selectin-dependent rolling on a variety of ligands (5, 6, 27). The number of rolling cells peaked at 1.25 dyn/cm^2 and then gradually declined as wall shear stress was increased further. Like P-selectin L1–2 cells, the L-selectin L1–2 cells rolled on the construct in which Thr-57 was replaced with Ser but not on the construct in which Thr-57 was replaced with Ala. These data strongly suggest that PSGL-1 must express a critical O-glycan at a Ser or Thr at position 57 to interact with P- and L-selectin.

At all wall shear stresses studied, comparable numbers of P-selectin L1–2 cells rolled on wild-type PSGL-1 and on each construct in which two of the three Tyr residues were substituted with Phe (Fig. 2*C*). P-selectin L1–2 cells did not roll on the PSGL-1 construct in which all three Tyr residues were substituted with Phe, confirming previous studies (16). L-selectin L1–2 cells also rolled on all three single-Tyr PSGL-1 constructs but not on the construct lacking all three Tyr residues (Fig. 2*D*). However, rolling L-selectin L1–2 cells required slightly higher wall shear stresses to accumulate on the single-Tyr constructs than on wild-type PSGL-1, with accumulation peaking at 2 dyn/cm^2. To further compare the adhesive properties of wild-type and single-Tyr forms of PSGL-1, cells expressing P- or L-selectin were allowed to accumulate on transfected CHO cell monolayers at 0.5 or 1.0 dyn/cm^2, respectively, and then subjected to incremental increases or decreases in wall shear stress. P-selectin L1–2 cells detached slightly faster from single-Tyr than wild-type PSGL-1 at higher wall shear stress. L-selectin L1–2 cells detached comparably from wild-type and single-Tyr PSGL-1 as wall shear stress was decreased or increased from optimal levels (data not shown). The rate that P- or L-selectin L1–2 cells tethered to wild-type and single-Tyr PSGL-1 was also similar at all wall shear stresses examined (Fig. 3). These results demonstrate that PSGL-1 requires only a single Tyr to support

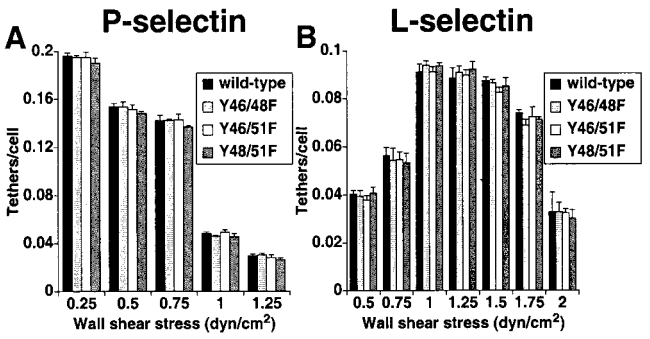

Fig. 3. Rate of tethering of cells expressing P- or L-selectin to wild-type or single-Tyr PSGL-1. Cells expressing P-selectin (*A*) or L-selectin (*B*) were perfused over each PSGL-1 construct at the indicated wall shear stress. The number of cells that tethered to the monolayer over a 30-s interval was quantified and normalized by dividing by the number of cells delivered across the field of view in the focal plane of the monolayer. The data represent the mean ± SD of four experiments.

tethering and rolling of cells expressing either P- or L-selectin. However, examination of the videotapes indicated that P- or L-selectin L1–2 cells tended to roll more irregularly on single-Tyr than wild-type PSGL-1. This prompted us to examine more closely the parameters of selectin-dependent rolling on these constructs.

Kinetics of Rolling of P- and L-Selectin L1–2 Cells on Wild-Type or Single-Tyr PSGL-1. We used specialized software to track the displacements of multiple cells rolling on wild-type or single-Tyr PSGL-1 between two successive video frames. Each displacement was divided by the time interval of 0.033 s to derive the velocity. Fig. 4 *A* and *B* shows the velocity at each frame for a representative P-selectin- or L-selectin L1–2 cell rolling on wild-type PSGL-1 at 1 dyn/cm^2. The P-selectin L1–2 cell rolled much slower and had much smaller fluctuations in rolling velocity than the L-selectin L1–2 cell.

To examine the stability of rolling, we determined the distribution of distances traveled between pauses for many P- or L-selectin L1–2 cells rolling on wild-type or single-Tyr PSGL-1 over a range of wall shear stresses. Fig. 4 *C* and *D* illustrates the distributions of distances traveled for P- and L-selectin L1–2 cells on the PSGL-1 constructs at 1 dyn/cm^2. Most P- or L-selectin L1–2 cells had relatively short travel distances on wild-type or single-Tyr PSGL-1. P-selectin L1–2 cells had fewer long travel distances, and the longest ones were generally slightly greater than 10 μm. L-selectin L1–2 cells had a much broader range of travel distances, including a significant percentage >28 μm. Whereas some short travel distances may result from stretching of microvillus tethers (28), long travel distances more likely result from breakage of selectin-PSGL-1 bonds at the rear edge of the cell. We therefore compared the percentages of large travel distances, i.e., >10 μm for P-selectin and >28 μm for L-selectin, on wild-type and single-Tyr PSGL-1 constructs over a range of wall shear stresses (Fig. 4 *E* and *F*). The P-selectin L1–2 cells had significantly more large travel distances on single-Tyr PSGL-1, particularly on the Y46/51F and Y48/51F constructs, than on wild-type PSGL-1 at all wall shear stresses studied (Fig. 4*E*). L-selectin L1–2 cells had many more large travel distances on single-Tyr than wild-type PSGL-1 at low shear, but these differences disappeared as shear was increased (Fig. 4*F*). P- and L-selectin L1–2 cells also rolled with higher mean velocity and greater variance of velocity on single-Tyr than wild-type PSGL-1 (data not shown). These quantitative data support the observation that P- and L-selectin L1–2 cells rolled more irregularly on single-Tyr than wild-type PSGL-1. For

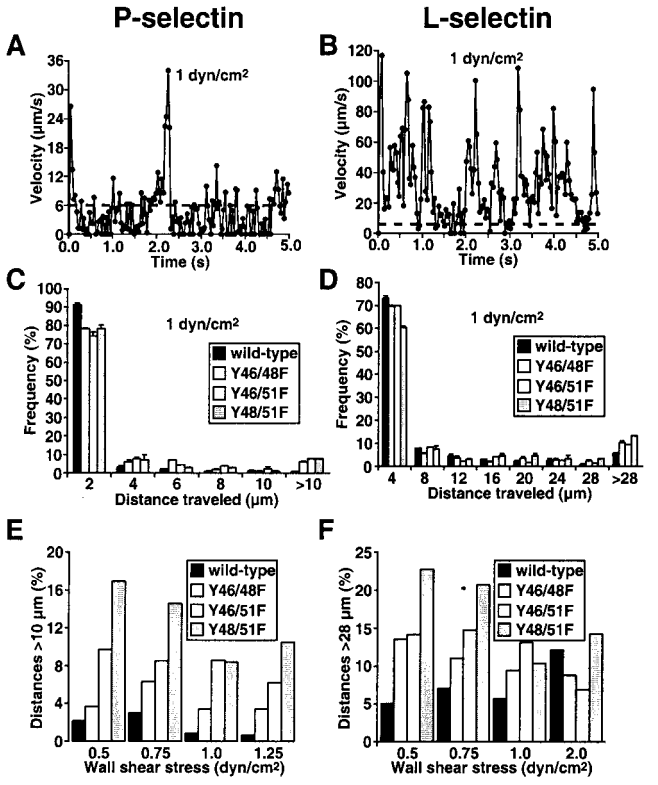

Fig. 4. Kinetics of rolling of cells expressing P- or L-selectin on wild-type or single-Tyr PSGL-1. (*A* and *B*) Frame-by-frame velocities of representative L1–2 cells expressing P- or L-selectin rolling on wild-type PSGL-1 at 1 dyn/cm^2. The dashed line represents the velocity threshold used to separate paused from rolling cells. (*C* and *D*) Distribution of travel distances for cells rolling on wild-type or single-Tyr PSGL-1 at 1 dyn/cm^2. At least 20 L1–2 cells were tracked for up to 5 s for a total observation time of ≥100 s. The travel distance of a rolling cell was defined as the distance spanned during one continuous sequence of velocities >6 μm/s. The bars represent an estimate of the cumulative error for the measurements. (*E* and *F*) Frequency of large distances traveled (>10 μm for P-selectin or >28 μm for L-selectin) for L1–2 cells rolling on wild-type or single-Tyr PSGL-1 as a function of wall shear stress.

P-selectin, the differences between wild-type and single-Tyr PSGL-1 persisted at shears from 0.5 to 1.25 dyn/cm^2, whereas for L-selectin, the differences disappeared as shear was increased from 0.5 to 2 dyn/cm^2.

Kinetics of Dissociation and Mechanical Strength of Transient Tethers of P- or L-Selectin with Wild-Type or Single-Tyr PSGL-1. The altered kinetics of rolling of P- or L-selectin L1–2 cells on wild-type vs. single-Tyr PSGL-1 could represent differences in the association or dissociation rates of selectin–PSGL-1 bonds. The tethering rates, which primarily reflect k_{on} rather than k_{off}, were indistinguishable on wild-type and mutant PSGL-1 (Fig. 3). We therefore measured the dissociation rates of transient tethers, which may represent single adhesive bonds. CHO cell monolayers were preincubated with a subsaturating concentration of anti-PSGL-1 mAb PL1 that reduced the effective site density of PSGL-1 such that P- or L-selectin L1–2 cells formed transient tethers with the monolayer. These transient tethers represented specific selectin–PSGL-1 interactions, because they were eliminated by addition of a saturating concentration of PL1. The durations of transient tethers were measured in five independent experiments for each selectin–PSGL-1 interaction over a range of wall shear stresses. Fig. 5 *A* and *B* shows representative data at a single wall shear stress for P- or L-selectin, respectively. In the examples shown,

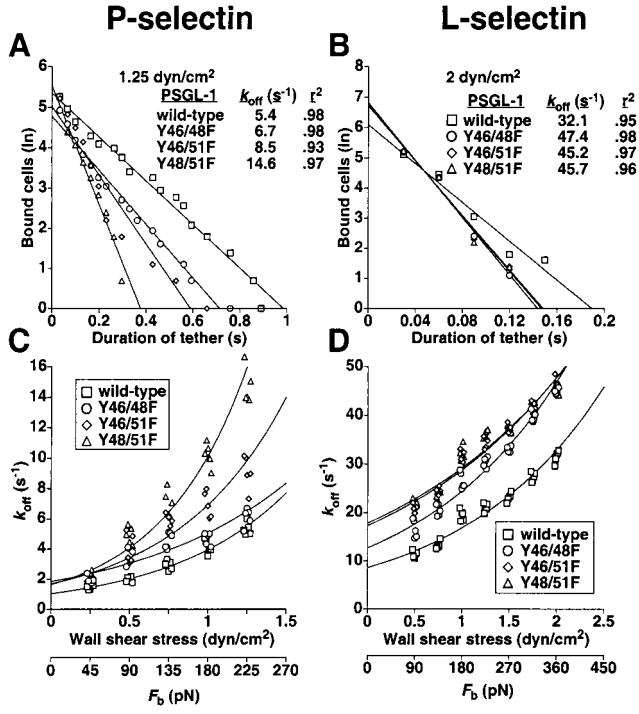

Fig. 5. Kinetics of dissociation and mechanical strength of transient tethers of P- or L-selectin-expressing cells to wild-type or single-Tyr PSGL-1. (*A* and *B*) Representative first-order dissociation kinetics for transient tethers of L1–2 cells expressing P- or L-selectin to each PSGL-1 construct at the indicated wall shear stress. For each set of tether lifetimes, the line is the least squares fit, and the slope is $-k_{off}$ for the selectin–PSGL-1 bond. (*C* and *D*) Effect of increased wall shear stress and force on the tether bond on dissociation kinetics of P- or L-selectin with wild-type or single-Tyr PSGL-1. Each group of points represents a single wall shear stress from each of five independent experiments. The points were displaced horizontally so that all points could be seen. The data were fit to the Bell equation (24).

the k_{off} of P- or L-selectin was greater for the single-Tyr PSGL-1 constructs than for wild-type PSGL-1.

The measured dissociation rates were plotted against wall shear stress, and the data were fit to a theoretical relationship between k_{off} and the force on the tether bond, F_b (Fig. 5 *C* and *D*). The fit yielded values for k^0_{off}, i.e., the k_{off} in the absence of force, and for a, the reactive compliance, which is inversely proportional to the mechanical stability of the tether bond (Table 1). The values for k^0_{off} and a for interactions of P- and L-selectin with wild-type PSGL-1 were in good agreement with published values for interactions of P- and L-selectin with PSGL-1 on neutrophils (4, 6). The k^0_{off} was not clearly distinguishable for the interaction of P-selectin with wild-type PSGL-1 and each single-Tyr form of PSGL-1. However, the tether dissociation rates increased much more on two of the single-Tyr constructs (Y46/51F and Y48/51F) than on wild-type PSGL-1 in response to higher wall shear stress. In marked contrast, the k^0_{off} was higher for the interaction of L-selectin with each single-Tyr construct than for wild-type PSGL-1, but the susceptibility of the tether dissociation rate to increasing wall shear stress was similar on wild-type and mutant PSGL-1. The statistical significance of the observed differences was independently confirmed by nonlinear regression analysis and by the method of maximum likelihood (26). These results demonstrate that substitutions of Tyr residues in PSGL-1 impair the mechanical strength, but not the unstressed k_{off}, of the P-selectin bond, whereas they increase the unstressed k_{off}, but not the mechanical strength, of the L-selectin bond.

Table 1. Dissociation rates and reactive compliance values for P- and L-selectin bonds with PSGL-1 constructs

	PSGL-1	k^0_{off} (s^{-1})	a (Å)
P-selectin	Wild-type	1.1 ± 0.1	0.29 ± 0.02
	Y46/48F	1.8 ± 0.1	0.24 ± 0.02
	Y46/51F	1.7 ± 0.2	0.33 ± 0.03
	Y48/51F	1.6 ± 0.2	0.42 ± 0.04
L-selectin	Wild-type	8.6 ± 0.4	0.16 ± 0.01
	Y46/48F	12.7 ± 1.1	0.15 ± 0.01
	Y46/51F	17.3 ± 0.4	0.12 ± 0.00
	Y48/51F	18.3 ± 0.5	0.11 ± 0.00

Values for k^0_{off} and a were derived from Fig. 5 *C* and *D*. The data represent the mean ± SD of five experiments.

Discussion

P- and L-selectin bind to sialylated and fucosylated glycoconjugates, such as sLe^x, and also interact with certain classes of sulfated glycoconjugates. The leukocyte mucin, PSGL-1, combines a group of three Tyr-SO_3 residues with a core-2-based O-glycan terminating in sLe^x into an N-terminal binding site for P-selectin. The data presented here indicate that the same modifications constitute a binding site for L-selectin. PSGL-1 required at least one of three clustered Tyr residues at residues 46, 48, and 51, plus a critical O-glycan attached to a Thr or Ser at residue 57, to bind to L-selectin and P-selectin. Despite these similarities, P- and L-selectin bound to recombinant PSGL-1 with distinct kinetic and mechanical features, as observed previously for other ligands (5, 6, 27). Compared with P-selectin, L-selectin required a shear threshold for both tethering and rolling adhesion, mediated faster and more irregular rolling, and dissociated much faster from PSGL-1. However, the L-selectin–PSGL-1 bond had greater mechanical strength than the P-selectin–PSGL-1 bond, as manifested by a smaller increase in k_{off} in response to force applied to the tether bond.

At the densities used, rolling cells expressing P- or L-selectin accumulated on the single-Tyr forms of PSGL-1 at or near the levels observed on wild-type PSGL-1. Closer examination, however, revealed that rolling was less stable on single-Tyr PSGL-1, particularly at lower wall shear stresses (Fig. 4 *E* and *F*) or at lower PSGL-1 densities (V.R. and R.P.M., unpublished data). Cells rolled more irregularly on single-Tyr PSGL-1, which was quantified as a higher percentage of large distances traveled between pauses. This could result from a slower association rate and/or a faster dissociation rate for bonds. Cells expressing P- or L-selectin tethered at similar rates on wild-type and single-Tyr PSGL-1. Because the tethering rate primarily reflects k_{on}, the data suggest that a slower association rate is not the principle reason for less stable rolling.

Unlike the lack of differences in tethering rates, clear abnormalities were noted in the tether lifetimes of P- or L-selectin with the single-Tyr forms of PSGL-1. These results revealed that the unstressed k_{off}, or k^0_{off}, for the bond with P-selectin was indistinguishable for wild-type and single-Tyr PSGL-1. However, the mechanical stability of the P-selectin bond was significantly impaired for two of the single-Tyr constructs. In marked contrast, the k^0_{off} of the L-selectin bond was significantly higher for all three single-Tyr forms of PSGL-1 than for wild-type PSGL-1, yet the mechanical stabilities of all L-selectin–PSGL-1 bonds were similar. Using the equation of Goldman *et al.* (25), we modeled a uniform relationship between wall shear stress and the force on the tether bond, F_b. A pulling force on PSGL-1 causes neutrophils to lengthen their microvilli or to extrude membrane tethers from the microvilli, which would lessen the actual force on the tether bond in shear flow (28). If L1–2 cells expressing selectins or CHO cells expressing PSGL-1 also ex-

trude membrane tethers, the values for F_b would be lower than those estimated, especially at higher wall shear stress, but the differences in k_{off} between wild-type and single-Tyr PSGL-1 would persist. The principle effect of the mutations is probably to reduce the average number of Tyr-SO_3 residues from three to one per subunit of PSGL-1, although other structural alterations induced by substitution of two Phe residues for two Tyr residues cannot be excluded. The ability to synthesize synthetic glycosulfopeptides in which sulfation can be precisely controlled will provide a more definitive assessment of how the stoichiometry and positioning of Tyr-SO_3 affects the interaction of PSGL-1 with P- and L-selectin (17).

It has been suggested that higher wall shear stress stabilizes leukocyte rolling by increasing formation of selectin–ligand bonds, which compensates for the exponential increase in dissociation rates of these bonds (29). This might explain why P- or L-selectin-expressing L1–2 cells rolled more smoothly and with fewer long travel distances as shear was increased. An increase in formation of selectin bonds might also explain why the instability of cells rolling on single-Tyr relative to wild-type PSGL-1 did not worsen at higher shears. Indeed, the stability of cells rolling through L-selectin on single-Tyr PSGL-1 approached that on wild-type PSGL-1 as shear was increased from 0.5 to 2 dyn/cm^2. Shear-enhanced bond formation may be more likely during rolling than during tethering, because tethering rates were the same on wild-type and single-Tyr PSGL-1 at any given wall shear stress. We attempted to quantify individual rolling steps, a putative measure of the dissociation rate of discrete bond clusters at the trailing edge of the cell, and a potential tool for modeling the number of selectin bonds (29). However, we found that the temporal and spatial resolution of the videomicroscopy system did not allow accurate distinction of individual rolling steps, and small changes in the definition of a pause led to large differences in estimates for pause times of putative single steps. Each such step may actually represent two or more discrete adhesive steps that cannot be resolved, although video cameras that operate at a higher frame speed might increase resolution. We therefore used a more conservative estimate of rolling cell displacement, the distance in which a cell traveled continuously at a velocity above that of a stationary cell.

The structural basis for the kinetic and mechanical features of selectin–ligand interactions is not known. Our studies show that two selectins bind to the same region of a mucin ligand but with different kinetic and mechanical properties that can be further distinguished by limited tyrosine replacements in the binding site of the mucin. It will be important to correlate these measurements made in shear flow with biochemical measurements that estimate the kinetics and affinity of binding in the absence of applied force. Determination of the three-dimensional structures of P- and L-selectin bound to a glycosulfopeptide modeled after the N-terminal region of PSGL-1 may help explain the remarkable properties of these interactions.

We thank Cindy Carter and Michael McDaniel for technical assistance and Kelsey Kennedy for computer support. This work was supported by National Institutes of Health Grant HL 54304. V.R. is the recipient of a postdoctoral fellowship from the Heartland Affiliate of the American Heart Association.

1. McEver, R. P., Moore, K. L. & Cummings, R. D. (1995) *J. Biol. Chem.* **270,** 11025–11028.
2. Kansas, G. S. (1996) *Blood* **88,** 3259–3287.
3. Lawrence, M. B. & Springer, T. A. (1991) *Cell* **65,** 859–873.
4. Alon, R., Hammer, D. A. & Springer, T. A. (1995) *Nature (London)* **374,** 539–542.
5. Alon, R., Chen, S. Q., Puri, K. D., Finger, E. B. & Springer, T. A. (1997) *J. Cell Biol.* **138,** 1169–1180.
6. Alon, R., Chen, S., Fuhlbrigge, R., Puri, K. D. & Springer, T. A. (1998) *Proc. Natl. Acad. Sci. USA* **95,** 11631–11636.
7. Puri, K. D., Chen, S. & Springer, T. A. (1998) *Nature (London)* **392,** 930–933.
8. McEver, R. P. & Cummings, R. D. (1997) *J. Clin. Invest.* **100,** 485–492.
9. Moore, K. L., Patel, K. D., Bruehl, R. E., Fugang, L., Johnson, D. A., Lichenstein, H. S., Cummings, R. D., Bainton, D. F. & McEver, R. P. (1995) *J. Cell Biol.* **128,** 661–671.
10. Walcheck, B., Moore, K. L., McEver, R. P. & Kishimoto, T. K. (1996) *J. Clin. Invest.* **98,** 1081–1087.
11. Sako, D., Chang, X.-J., Barone, K. M., Vachino, G., White, H. M., Shaw, G., Veldman, G. M., Bean, K. M., Ahern, T. J., Furie, B., *et al* (1993) *Cell* **75,** 1179–1186.
12. Wilkins, P. P., Moore, K. L., McEver, R. P. & Cummings, R. D. (1995) *J. Biol. Chem.* **270,** 22677–22680.
13. Sako, D., Comess, K. M., Barone, K. M., Camphausen, R. T., Cumming, D. A. & Shaw, G. D. (1995) *Cell* **83,** 323–331.
14. Pouyani, T. & Seed, B. (1995) *Cell* **83,** 333–343.
15. Li, F., Wilkins, P. P., Crawley, S., Weinstein, J., Cummings, R. D. & McEver, R. P. (1996) *J. Biol. Chem.* **271,** 3255–3264.
16. Liu, W.-J., Ramachandran, V., Kang, J., Kishimoto, T. K., Cummings, R. D. & McEver, R. P. (1998) *J. Biol. Chem.* **273,** 7078–7087.
17. Leppanen, A., Mehta, P., Ouyang, Y.-B., Ju, T., Helin, J., Moore, K. L., van Die, I., Canfield, W. M., McEver, R. P. & Cummings, R. D. (1999) *J. Biol. Chem.* **274**, 24838–24848.
18. Spertini, O., Cordey, A.-S., Monai, N., Giuffre, L. & Schapira, M. (1996) *J. Cell Biol.* **135,** 523–531.
19. Natsuka, S., Gersten, K. M., Zenitas, K., Kannagi, R. & Lowe, J. B. (1994) *J. Biol. Chem.* **269,** 16789–16794.
20. Diacovo, T. G., Puri, K. D., Warnock, R. A., Springer, T. A. & Von Andrian, U. H. (1996) *Science* **273,** 252–255.
21. Von Andrian, U. H., Hasslen, S. R., Nelson, R. D., Erlandsen, S. L. & Butcher, E. C. (1995) *Cell* **82,** 989–999.
22. Kishimoto, T. K., Jutila, M. A., Berg, E. L. & Butcher, E. C. (1989) *Science* **245,** 1238–1241.
23. Geng, J.-G., Bevilacqua, M. P., Moore, K. L., McIntyre, T. M., Prescott, S. M., Kim, J. M., Bliss, G. A., Zimmerman, G. A. & McEver, R. P. (1990) *Nature (London)* **343,** 757–760.
24. Bell, G. I. (1978) *Science* **200,** 618–627.
25. Goldman, A. J., Cox, R. G. & Brenner, H. (1967) *Chem. Eng. Sci.* **22,** 653–660.
26. Bevington, P. R. & Robinson, D. K. (1992) *Data Reduction and Error Analysis for the Physical Sciences* (McGraw Hill, New York).
27. Finger, E. B., Puri, K. D., Alon, R., Lawrence, M. B., Von Andrian, U. H. & Springer, T. A. (1996) *Nature (London)* **379,** 266–269.
28. Shao, J. Y., Ting-Beall, H. P. & Hochmuth, R. M. (1998) *Proc. Natl. Acad. Sci. USA* **95,** 6797–6802.
29. Chen, S. Q. & Springer, T. A. (1999) *J. Cell Biol.* **144,** 185–200.
30. Li, F., Erickson, H. P., James, J. A., Moore, K. L., Cummings, R. D. & McEver, R. P. (1996) *J. Biol. Chem.* **271,** 6342–6348.